

Kinetic Model & Analysis for Pyrolysis of Waste Polystyrene Over Laumontite

Krishna Kant Kumar Singh, Dr.S.P.Singh

Department of Chemical Engineering, BIT, Sindri, Jharkhand, 828123

Abstract

Laumontite(NZ) has been studied as a catalyst in the degradation (Catalytic Thermolysis) of polystyrene (PS) at 400°C in a semi batch reactor. Its performance on the degradation was compared with HZSM-5, silica-alumina and also with thermal degradation (thermolysis). HNZ was as effective as HZSM-5 for the production of liquid oils with carbon numbers of C5-C12, without any severe deactivation. The main product of PS degradation was styrene for both thermolysis and catalytic thermolysis. Among the catalysts tested, silica-alumina showed the highest yield of ethylbenzene and the lowest one of styrene due to its mesopores. Increase in degradation temperature for HNZ resulted in a decrease of selectivity towards ethylbenzene and propylbenzene, but an increase of styrene selectivity with lower yield of styrene dimers. A kinetic analysis by thermo gravimetric analysis was also carried out using a dynamic model. It offered reliable kinetic parameters for the catalytic degradation of PS over HNZ. The apparent activation energy was found to be 360kJ/mol, and the catalytic degradation of PS followed first-order kinetics.

Keywords: Polystyrene; Catalytic thermolysis; Laumontite; TGA

1. Introduction

Though various kinds of techniques have been proposed for the conversion of waste plastics, it is generally accepted that material recovery is not a long term solution to the present problem, and that energy or chemical recovery is a more attractive one. Consequently, new technologies are being investigated for the chemical recycling of plastic wastes. One approach is to employ inert gas thermolysis to produce gasoline-like materials. In this method, the waste plastics are thermally or catalytically degraded into gases and oils, which can be used as sources in fuels or chemicals [1].

Thermal degradation (thermolysis) of waste plastics into fuel oils was studied extensively, but the oils obtained showed a wide-ranged distribution of carbon atom numbers and contained a significant fraction of olefins [2–4]. The olefins are not favorable for fuel oils because these are easily polymerized into unusable compounds during storage and transportation. In contrast, the oils produced by catalytic degradation (catalytic thermolysis) are known to contain a relatively narrow distribution of hydrocarbons, lower amount of olefins and higher amount of aromatics compared to the oils from the thermal degradation. An excellent summary of the catalytic recycling of polymers was reported by Uemichi [2].

Tomar S.S. et al., reported maximum yield of liquid when polymer catalyst ratio was 4:1 and after this ratio the liquid yield decreases. The degradation of waste plastic was over two commercial grade cracking catalysts, HZY (20) & HZY (40) in a semi-batch reactor [3]. The most commonly used catalysts in the catalytic degradation of polymers are solid acids and bases [4–9].

Plastic wastes for the catalytic degradation processes are mainly limited to polyolefinic wastes (polyethylene and polypropylene) and polystyrene (PS). In contrast to polyethylene and polypropylene, PS can be thermally depolymerized to obtain the monomer styrene with a high selectivity. Zhang et al., [10] Obtained a styrene yield of 70 wt. % by PS degradation at 350°C using a semi-batch reactor with a continuous flow of nitrogen. On the contrary, Audisio et al. [11] reported very low selectivity (< 5 wt. %) to the styrene in PS degradation with solid acids such as silica-alumina and HY or REY zeolites at 350°C. The main products in their study were benzene, ethylbenzene and cumene. Ueki et al. [7] reported that solid bases, especially BaO, were more effective catalysts than solid acids (HSM-5 and silica-alumina) for the degradation of PS to styrene monomer and dimer at 350°C.

During the last two decades, thermogravimetric analysis (TGA) has been continuously used to understand the reaction mechanism of thermal degradation of polymers [12–14]. The degradation studies using TGA can offer valuable information's on the activation energy, the overall reaction order and the pre-exponential factor. Park et al., developed new mathematical methods for the kinetic analysis and reported a kinetic analysis of thermal degradation of polymer using a dynamic model, and compared this model to other methods. However, most of the previous works are related to thermal degradation of

polyethylene and polypropylene. There are only very few works are reported on the degradation of PS. The dynamic method has not get been applied for the catalytic degradation of PS.

Hwang EY et al., reported that the natural clinoptilolite zeolite was good catalyst for the degradation of polypropylene [5] and polyethylene [16]. The purpose of this study is to evaluate the performance of the natural zeolite (Laumontite) in the catalytic degradation of PS. The emphasis of this study is also placed on the kinetic analysis of catalytic degradation of PS. A dynamic model [15] was applied to predict the catalytic degradation of PS over NZ by TGA method.

2. Experimental (Materials and catalysts)

PS, in granular form, was collected from local market (Melt flow Index=7.5 g/10 min, density=1.03 g/cm³). The PS samples of 60-150 mesh size were used for this study. Several types of solid acid catalysts such as silica-alumina (Loba Chemie, India), ZSM-5 (Himedia Lab.) and Laumontite(NZ) was collected from local market. ZSM-5 and NZ were ion-exchanged three consecutive times with 1 M NH₄Cl solution for 20 h. The zeolites exchanged with NH₄⁺ were dried at 110°C for 6 h, and then calcined in air at 400°C to obtain the proton (H⁺) exchanged zeolites like HZSM-5 and HNZ.

3. Apparatus and procedure

The catalytic thermolysis of PS was carried out in a semi-batch reactor. The thermolysis setup used in this experiment is shown in Figure 1. It consists of a semi batch reactor (steel made) of volume 2 liters, vacuum-packed with two outlet tubes towards vacuum pump and condenser. Vacuum pump with a gage is attached to the reactor so as carryout the reaction in vacuum. The condenser is attached to collect condensed Liquid hydrocarbons and gases separately. The reactor is heated externally by an electric furnace, with the temperature being measured by a Cr-Al: K type thermocouple fixed inside the reactor, and temperature is controlled by an external PID controller. 100 gm of waste plastics sample were loaded in each thermolysis reaction. The condensable liquid products was collected through the condenser and weighed. After thermolysis, the solid residue left inside the reactor was weighed. Then the weight of gaseous/volatile product was calculated from the material balance. The uncondensed gases were separated out in a bladder from condenser. Apparatus setup and samples for testing are shown in Fig. 1(a, b).



Figure 1(a) Apparatus setup

The kinetics of PS degradation at non-isothermal conditions has been investigated using TGA at various heating rates between 10 and 50°C/min. The initial weight of PS sample was 100 gm and that of HNZ catalyst was 10 gm. The experiments were carried out in vacuum.

3.1 Analysis

The bulk structure of the NZ was confirmed by XRD analysis with Cu-Kα radiation. The composition of the NZs was determined by atomic absorption spectroscopy (Perkin-Elmer AAS 5100). The acidic properties of the catalysts were determined by a conventional temperature programmed desorption experiment of ammonia in the temperature range of 100 to 700°C at a constant heating rate of 5°C/min. The specific surface area and pore size of the catalysts were measured by a BET apparatus.

The degradation of the PS gave off gases, liquids and residues. The residue means the carbonaceous compounds remaining in the reactor and deposited on the wall of the reactor. The amount of coke deposit on the catalyst was calculated by measuring the desorbed amount of carbon dioxide during temperature programmed oxidation of used catalysts. The gases were analyzed by GC. The condensed liquid samples were analyzed by GC-MS. The physical properties and the composition of the liquids were also measured.



Figure 1(b) Samples for testing

3.2 Kinetic analysis

In the kinetics of polymer degradation using TGA, it is very common to use the basic rate equation of conversion α for thermal degradation in inert atmosphere [15] as

$$\frac{d\alpha}{dt} = A(1 - \alpha)^n \exp\left(\frac{-E}{RT}\right) \quad (1)$$

where A is pre-exponential factor (l/min), E is the activation energy (J/mol), T is the temperature of reaction (K) and R is the gas constant (8.314 J/mol K), and n denotes the overall reaction order. However, A is not strictly constant but depends, according to collision theory [17], on $T^{0.5}$. Therefore, if the basic Eq. (1) is taken and a heating rate $\beta = dT/dt$ (K/min) is employed, it can be shown that

$$\frac{d\alpha}{dT} = \frac{A_0}{\beta} = T^{1/2} \exp\left(-\frac{E}{RT}\right) (1-\alpha)^n \quad (2)$$

If the temperature rises at a constant heating rate β , and the kinetic parameters at any weight loss fraction are approximately equal to those of its neighboring weight loss fraction, then by differentiation of Eq. (2), Eq. (3) can be obtained.

$$\frac{d^2\alpha}{dT^2} = \frac{1}{\beta} \left(\frac{d\alpha}{dT} \right) \left[n(1-\alpha)^{-1} \left(-\frac{d\alpha}{dT} \right) + \frac{E}{RT^2} + \frac{1}{2} T^{-1} \right] \quad (3)$$

The maximum degradation rate occurs when $d^2\alpha/dT^2$ is zero. Therefore, Eq. (3) at maximum rate gives

$$\begin{aligned} & \frac{A_0}{\beta} T_{max}^{1/2} \exp(-E/RT_{max}) n(1-\alpha_{max})^{n-1} \\ &= \frac{-E}{RT_{max}^2} + \frac{1}{2} T_{max}^{-1} \end{aligned} \quad (4)$$

where T_{max} (maximum peak temperature) and α_{max} (weight loss fraction at the peak temperature). Using Murray and White's expression [18], integration of Eq. (2) results in,

$$\begin{aligned} & \frac{1}{n-1} \left[\frac{1}{(1-\alpha)^{n-1}} - 1 \right] \\ &= \frac{A_0 R}{\beta E} T^{5/2} \left(1 - \frac{5RT}{2E} \right) \times \exp(-E/RT) \end{aligned} \quad (5)$$

If Eq. (4) is combined with Eq. (5), the following result is obtained:

$$n(1-\alpha_{max})^{n-1} = n - (n-1) \left(1 + \frac{RT_{max}}{2E} \right) \approx 1 \quad (6)$$

Eq. (6) does not contain the heating rate β except as T_{max} varies with heating rate. The product $n(1-\alpha_{max})^{n-1}$ is not only independent of β , but is very nearly equal to unity. By substituting this value in Eq. (4) and taking the natural logarithm, one obtains:

$$\ln \beta = \ln A_0 + \frac{2}{3} \ln T_{max} - \ln \left(\frac{E}{RT_{max}} + \frac{1}{2} \right) - \frac{E}{RT_{max}} \quad (7)$$

The plot of $\ln \beta$ versus $1/T_{max}$ should give a straight line with the slope $-E/R$ giving the activation energy E at maximum rate, and A_0 can be calculated from the activation energy E and the intercept on the Y axis [19]. Eqs. (2) and (3) give the following expressions for n and E .

$$n = \frac{\left[\beta \left(\frac{d^2\alpha}{dT^2} \right) / \left(\frac{d\alpha}{dT} \right) - \frac{E}{RT^2} - \frac{1}{2} T^{-1} \right] (1-\alpha)}{\left(-\frac{d\alpha}{dT} \right)} \quad (8)$$

$$E = RT \ln \left[\frac{\left(\frac{d\alpha}{dT} \right)}{A_0 T^{1/2} (1-\alpha)^n} \right] \quad (9)$$

If the factor A_0 is determined, the n and E values at any weight loss fraction can be obtained from Eqs. (8) and (9) by numerical methods. The average reaction order and activation energy can be calculated from Eqs. (10) and (11) as the followings:

$$n_{ave} = \frac{\sum_{i=1}^N n_i (\alpha_i - \alpha_{i-1})}{\alpha_f} \quad (10)$$

$$E_{ave} = \frac{\sum_{i=1}^N E_i (\alpha_i - \alpha_{i-1})}{\alpha_f} \quad (11)$$

where α_f is the final weight loss fraction and N denotes the total number of TG data.

4. Results and discussion

4.1 Characterization of catalysts

Table 1				
Catalyst	Structure	Pore size (Å)	Si/Al ratio	S _{BET} (m ² /g)
HNZ ^a	Laumontite	7.6 X 30 3.3 X 4.6	4	271
SA	Amorphous	60-100	13% Al ₂ O ₃	504
HZSM-5	MFI	5.3X5.6 5.1X5.5	22	417

^a Relative weight ratio of other metal components based on Al is as follows; Si=4.0, Na=0.21, K=0.08, Ca=0.02, Ti=0.01, Fe=0.03.

The main physicochemical properties of the catalysts used in the PS degradation are shown in Table 1. The HNZ is a silicrich member of the Laumontite family [20]. Its porestructure is characterized by two main channels parallel to the c -direction, one formed by a 10-member ring (7.6 X 3.0 Å) and the other by an eight-member ring (3.3~4.6 Å). BET analysis on pore volume distribution in Fig. 2 shows that most of pores in HNZ are micro-pores of about 5 Å, and it has practically no mesopores. The total pore volume of pores between 4.5 to 9.1 Å is 0.11 cm³/g. Silica-alumina has a wide-range mesopores with surface area of 504 m²/g. HZSM-5 has Si/Al ratio of 22 and surface area of 417 m²/g.

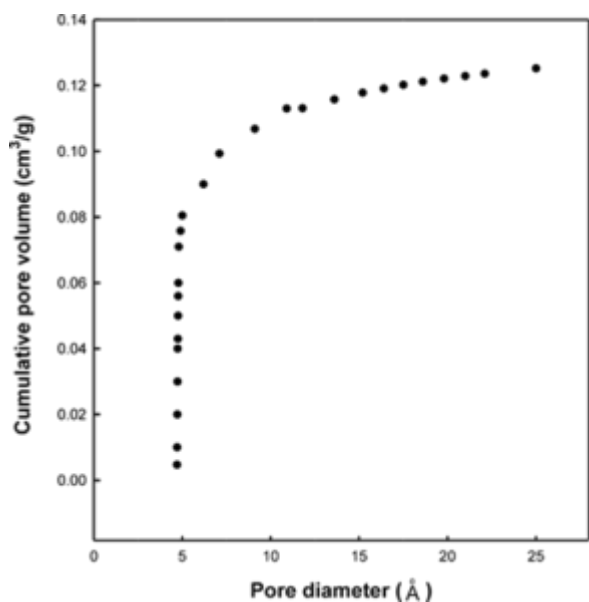


Figure 2. Cumulative pore volume distribution of HNZ.

4.2 Degradation of PS

PS, alone or together with catalysts (HNZ, HZSM-5, SA) in the reactor, was degraded at 400°C for 2 h. Table 2 lists the gases, liquids, residues and cokes on the catalyst from the degradation experiment. The amount of gases products was calculated by subtracting the sum of weights for liquids, residues and catalyst with coke, from the total weight of PS sample and fresh catalyst initially loaded to the reactor. Carbonaceous compounds adhering to the reactor wall were dissolved in *n*-hexane and were measured as degradation residues. In all cases, the liquid oils were main products. The HNZ showed a comparable performance with SA in producing liquid oils for the degradation of PS without producing much residues and cokes.

HZSM-5 catalyst has a MFI structure with intersecting 5.3 X 5.6 and 5.1 X 5.5 Å channels [21]. Therefore, the initially cracked fragments can diffuse through the pores of HZSM-5 and react further in the cavities created at the intersection of two channels, yielding more gaseous products.

Catalyst	Contents of products (wt.%)			
	Gases	Liquids	Residues	Cokes
Thermal	8.5	81.7	9.8	–
HNZ	9.7	81.5	4.9	3.9
HZSM-5	14.7	75.1	6.3	3.9
SA	7.7	83.5	4.8	4.0

Product distribution in the degradation of PS at 400°C for 2 h

The distributions of liquid products by carbon atom number obtained in both thermolysis and catalytic thermolysis are shown in Fig. 3. The main products are C₈ hydrocarbons, with C₉ and C₇. The hydrocarbons of C₁₄ or higher, mainly dimers of styrene and small amount of trimers, are 14-15 wt.% for thermal degradation and for HNZ. However, those for HZSM-5 and SA are 27-28 wt.%. These results are different from the ones obtained in the catalytic thermolysis of polyethylene or polypropylene, where the use of HNZ, HZSM-5 and SA catalysts shows no formation of hydrocarbons for C₁₄ or higher [5, 16].

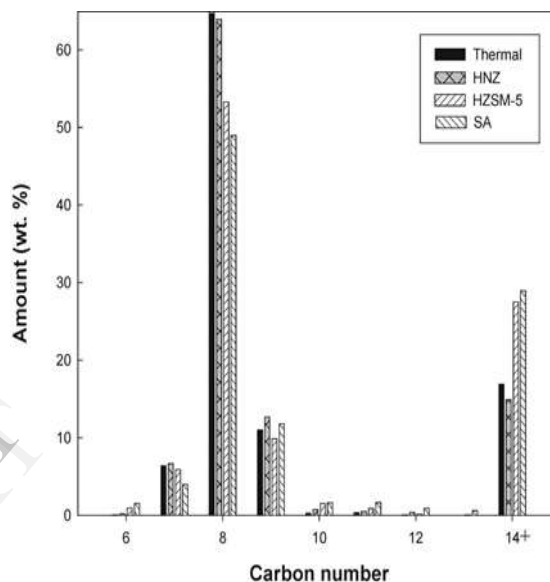


Figure 3. Product distribution of liquid formed in the degradation of PS over H-form catalysts and SA at 400°C.

Table 3 shows the distribution of liquid products by hydrocarbon type. Both thermolysis and catalytic thermolysis showed only aromatic compounds, since they are stable enough not to be further cracked or hydrogenated to paraffins or olefins. Only silica-alumina shows very small amount of isoparaffins. The main products, aromatic hydrocarbons, are identified in detail as shown in Table 4. Thermal degradation shows the highest amount of styrene (70.1 wt.%) and the lowest amount of ethylbenzene (8.8 wt.%). Thermolysis degradation of PS starts with a random initiation to form polymer radicals [22], the main products being styrene and its corresponding dimers and trimers.

Catalyst	Distribution of liquid (wt.%)				
	n-Paraffins	iso-Paraffins	Olefins	Naphthenes	Aromatics
Thermal	0.01	0.27	0.24	0.27	99.21
HNZ	0.04	0.52	0.09	0.22	99.14
ZSM-5	0.02	0.2	0.13	0.22	99.42
SA	0.15	1.63	0.6	0.79	96.83

Distribution of liquid product in the degradation of PS at 400°C for 2 h

The catalytic degradation over amorphous SA exhibits the lowest amount of styrene (48.2 wt.%) with quite a big increase in the selectivity towards ethylbenzene(30.2 wt.%) and benzene (2.5 wt.%) compared to the degraded aromatic products for HNZ (styrene=60.1 wt.%, ethylbenzene=16.0 wt.%) and HZSM-5 (styrene=62.6 wt.%, ethylbenzene=13.0 wt.%). The same phenomena on the distribution of styrene and ethylbenzene are also reported by Serrano et al. [23] for the catalytic degradation of PS over SA and HZSM-5. They obtained 16 wt.% of styrene for SA and 50 wt.% of styrene for HZSM-5 after the PS degradation at 375°C for 30 min.

Table 4

Aromatics	Thermal	HNZ	HZSM-5	SA
Benzene	0.06	0.24	1.25	2.45
Toluene	7.73	7.93	7.85	6.34
Ethylbenzene	8.79	15.97	12.96	30.19
Xylene	0.02	0.03	0.17	0.02
Styrene	70.08	60.08	62.6	48.21
Isopropylbenzene	2.11	3.45	2.58	0.06
α -Methylstyrene	10.57	11.45	10.48	10.09
Trimethylbenzene	0.34	0.04	0.42	0.57
Indane	0.02	0.01	0.15	0.1
Indene	0.02	0.06	0.23	0.14
Butylbenzene	0.02	0.36	0.01	0.3
Methylpropylbenzene	0.09	0.2	0.07	1.09
Diethylbenzene	0.02	0.04	0.08	0.07
Dimethylethylbenzene	0.02	0.02	0.26	0.08
Tetramethylbenzene	0.04	0.02	0.39	0.06
Methylindane	0.01	0	0.04	0
Naphthalene	0.04	0.03	0.43	0.05
Methylnaphthalene	0	0.08	0.03	0.22

Composition of aromatic compounds (wt.%) formed in the degradation of polystyrene at 400°C for 2 h

The acid catalyzed cracking of PS is of carbenium nature [24]. The most likely reaction pathway involves the attack of proton associated with a Brønsted acid site to the aromatic rings of PS, due to the reactivity of its side phenyl groups towards electrophilic reagents. The resulting carbenium may undergo β -scission followed by a hydrogen transfer. The possible production pathways of benzene, styrene, methylstyrene, toluene, ethylbenzene, isopropylbenzene and indane derivatives are reported by Audisio et al. [11].

Alternatively, the protonated polymer backbone may proceed through cross-linking reactions among adjacent polymeric chains or even inside the same polymer [25]. Serrano et al. [23] reported that the cross-linking reactions were promoted by the strong Brønsted acid site of HZSM-5, and therefore it showed very low conversion in the cracking of PS at low temperature (below 375°C). They explained the low activity of silica-alumina for the cross-linking reactions and its high activity for the cracking reactions by its medium acid strength distribution with a large amount of Lewis acid site [26] and by its mesopores.

Benzene and ethylbenzene can also be formed by further cracking and hydrogenation of the product styrene. Therefore, their highest amounts for SA in Table 4 may be due to these reactions in mesopores of SA where styrene molecule can easily enter inside the mesopores. However, HNZ and HZSM-5 having micropores will have less opportunity for these reactions.

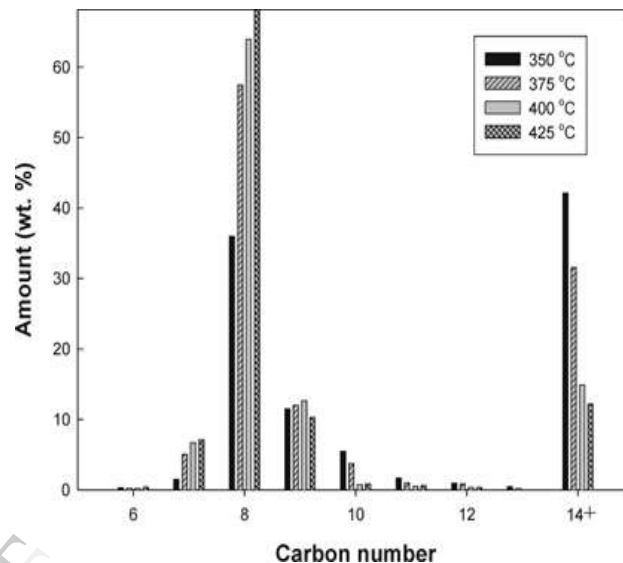


Figure 4. Effect of temperature on the distribution of liquid formed over HNZ.

The effect of temperature on the PS degradation was studied using HNZ catalysts over 350-425°C for 2 h. Table 5 shows the product distribution. At low temperatures the amount of residues for HNZ catalyst was high, 78.2 and 26.3 wt.% for 350 and 375°C, respectively. But at higher temperatures their amounts were very small. This indicates that the competitive cross-linking reactions take place first, especially at low temperatures; therefore the cracking of the resulting cross-linked polymer becomes harder. Even though the amount of liquid products varies much with temperature, the distributions of the liquids are compared to understand the degradation mechanism. Fig. 4 shows the distributions of liquid products by carbon atom number. The amount of C₈ hydrocarbon increases and that of C₁₄ and higher decreases with the increase of degradation rate.

Table 5

Temp.	Contents of products (wt. %)			
	Gases	Liquid	Residues	Cokes
350	5.3	9	78.2	7.5
375	7.2	61.4	26.3	5.1
400	9.7	81.5	4.9	3.9
425	9.4	84.4	3	3.2

Effect of temperature on the product distribution of PS degradation with HNZ for 2 h.

The distribution of aromatic hydrocarbons is shown

in Table 6. At 350°C indane is produced with an appreciable amount. It is interesting that the highest selectivity towards styrene is obtained at 425°C, with lowest selectivity to ethylbenzene and propylbenzene. Ethylbenzene and propylbenzene can be produced by inter-molecular hydride transfer of the corresponding polymer ion formed by β -scission of C-C bond in PS [11]. If the hydrogenation of the product styrene, faster at high temperature, occurs mainly to produce ethylbenzene, the temperature dependence of the amount of ethylbenzene and styrene in Table 6 will be inverted. Therefore, it may be concluded that the further cracking or hydrogenation of styrene are very hard to occur in HNZ having micropores. For the competitive pathways for styrene and ethylbenzene (or propylbenzene) productions, the latter seems favorable at lower temperature and the former at high temperature.

Aromatics	350 °C	375 °C	425°C	475 °C
Benzene	0.56	0.41	0.24	0.44
Toluene	2.74	5.48	7.93	8.34
Ethylbenzene	17.19	16.68	15.97	12.68
Xylene	0.05	0.03	0.03	0.01
Styrene	48.48	59.82	60.08	67.81
Isopropylbenzene	9.73	6.41	3.45	0.02
a-Methylstyrene	6.78	8.3	11.45	9.6
Trimethylbenzene	0.43	0.21	0.04	0.05
Indane	3.7	1.23	0.01	0.01
Indene	0.2	0.12	0.06	0.08
Butylbenzene	0.02	0.23	0.36	0.42
Methylpropylbenzene	0.23	0.22	0.2	0.05
Diethylbenzene	0.34	0.26	0.04	0
Dimethylethylbenzene	7.66	1.34	0.02	0
Tetramethylbenzene	0.12	0.04	0.02	0
Methylindane	0.4	0.12	0	0.03
Naphthalene	0.86	0.1	0.03	0.03
Methylnaphthalene	0.14	0	0	0.07

Composition of aromatics (wt.%) formed in the degradation PS at different temperatures

4.3 Kinetic studies on the PS degradation

The kinetic studies on the catalytic PS degradation over HNZ were carried out by TGA. Fig. 6 shows a typical TG curves at various heating rates. The symbols in this figures represent some of calculated values. It was found that the curves were displaced to higher temperatures due to the heat transfer lag and shorter contact time with increasing heating rate. Fig. 6 shows the plot of $\ln\beta$ vs. $1/T_{max}$. From the straight line the activation energy E at maximum degradation rate, and thus A_0 can be obtained at each heating rate from the intercept in Eq. (7). Then these A_0 values are substituted to Eq. (9) for the calculation of E and reaction order n by numerical method to solve Eq. (8)

and (9). The calculated average values of n_{ave} and E_{ave} are summarized in Table 7. However, average values of reaction order and activation energy are almost the same for all the different heating rates. The calculated values of weight loss fraction by using 4th order Runge-Kutta numerical integration are also presented in Fig. 6. It can be seen that the computed values agree very well with the TG data. From this kinetic study, the degradation of PS follows first-order reaction and apparent activation energy for the catalytic degradation of PS with HNZ is about 360kJ/mol. In a separate experiment of thermal degradation of PS with TGA, we obtained the apparent activation energy of about 380kJ/mol, higher than that of catalytic degradation. Audisio et al. [11] also reported the decrease of activation energy in the catalytic degradation of PS using Y zeolite and silica-alumina under vacuum. They used Freeman and Carroll's method [28] for the calculation of the apparent activation energy.

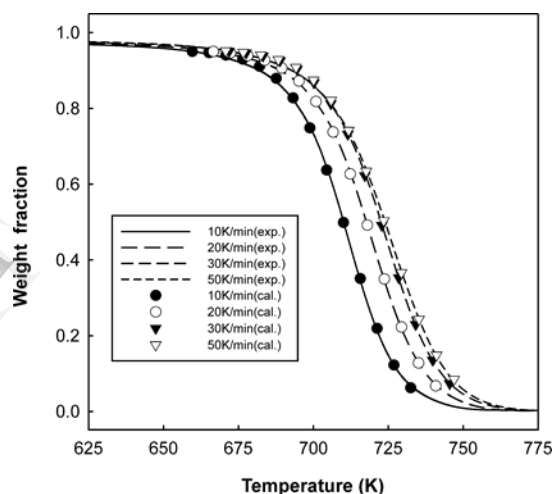


Figure 5. Comparison of TG curves of experimental and calculated data (symbols) for PS degradation with HNZ.

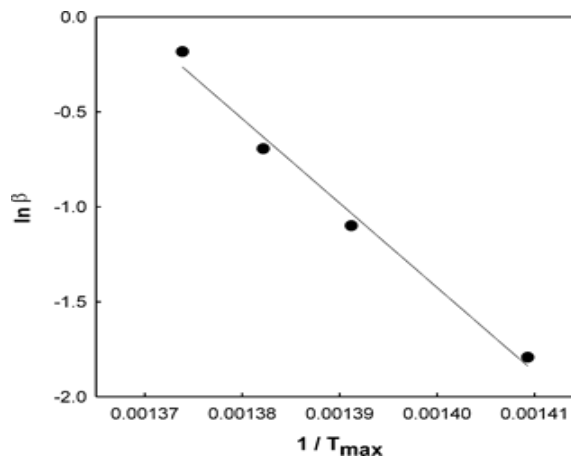


Figure 6. Plot of $\ln\beta$ versus $1/T_{max}$ for the determination of pre-exponential factor A_0 in the PS degradation with HNZ.

Table 7		
Heating rate, β (K/min)	Reaction order, n_{app}	Activation energy, E_{app}
10	1.01	359.0
20	1.01	360.8
30	1.00	361.3
50	1.02	361.0

Reaction order (n) and activation energy (E) for the degradation of polystyrene with HNZ

5. Conclusion

The natural Laumontite zeolite (HNZ) showed good catalytic performance for the catalytic degradation of PS, without much formation of residues or cokes at 400°C for 2 h. All the catalysts tested (HNZ, HZSM-5, SA) produced aromatic liquid oils with over 99% of selectivity. While styrene is the major product in both thermolysis and catalytic thermolysis over the solid acid catalysts, significant differences are observed in the aromatic products distribution. HNZ and HZSM-5 showed a decrease of styrene and an increased selectivity towards ethylbenzene and propylbenzene compared to thermal degradation. Amorphous Silica-alumina with ranges of mesopores showed the lowest amount of styrene and a big increase of ethylbenzene. Temperature increase shifted the carbon member distribution to lighter hydrocarbons. An increase of styrene monomer and a decrease of ethylbenzene and propylbenzene are observed for the PS degradation with HNZ. The kinetic analysis by TGA using a dynamic model explained well the catalytic thermolysis of PS over HNZ. The apparent activation for the reaction was 360kJ/mol, and the apparent reaction order was close to one.

References

- [1] Ohkita H, Nishiyama R, Tochihara Y, Mizushima T. *Ind Eng Chem Res* 1993; 32(12):3112.
- [2] Uemichi Y. *Catalysis (Japan)* 1995; 37(4):286.
- [3] Ahmad E., Chadar S., Tomar S.S., Akram M.K., *International Journal of Petroleum Science and Technology*, Vol. 3, No. 1, 25-34 (2009).
- [4] Mordi RC, Fields R, Dwyer J. *J Anal Appl Pyrol* 1994; 29:45.
- [5] Uemichi Y, Kashiwaya Y, Ayame A, Kanoh H. *Chem Lett* 1984:41.
- [6] Hwang EY, Choi JK, Kim DH, Park DW, Woo HC. *Korean J Chem Eng* 1998; 15(4):434.
- [7] Audisio G, Silivani A, Beltrame PL, Carniti P. *J Anal Appl Pyrol* 1984;7:83.
- [8] Ukei H, Hirose T, Horikawa S, Taka M, Azuma N, Ueno A. *Catal Today* 2000; 62:67.
- [9] Songip AR, Masuda T, Kuwahara H, Hashimoto K. *Appl Catal B: Environ* 1993; 2:153.
- [10] Zhang Z, Hirose T, Nishio S, Morioka Y, Azuma N,

Ueno A, et al. *Ind Eng Chem Res* 1995;34:4514.

[11] Audisio G, Bertini F, Beltrame PL, Carniti P. *Polymer Degrad, Stab* 1990;29:191.

[12] Petrovic ZS, Zavargo ZZ. *J Appl Poly Sci* 1986; 32:4353.

[13] Cooney JD, Day M, Wiles DM. *J Appl Polymer Sci* 1983; 28:2887.

[14] Deng BL, Chiu WY, Lim KF. *J Appl Polymer Sci* 1997; 66:1855.

[15] Park JW, Oh SC, Lee HP, Kim HT, Yoo KO. *Polymer Degrad Stab* 2000; 67:535.

[16] Park DW, Hwang EY, Kim JR, Choi JK, Kim YA, Woo HC. *Polymer Degrad Stab* 1999; 65:193.

[17] Turn SR. *An introduction to combustion: Concepts and application*. New York: McGraw-Hill, 1994.

[18] Murray F, White J. *Trans Br Ceram Soc* 1955; 54:151.

[19] Ozawa TJ. *Therm Anal* 1970;2:301.

[20] Woo HC, Lee KH, Lee JS. *Appl Catal A: General* 1996; 134:147.

[21] Mordi RC, Fields R, Dwyer J. *J Chem Soc Chem Communication* 1992: 374.

[22] Jellinek HG. *J Polymer Sci* 1949;4:13.

[23] Serrano DP, Aguado J, Escola JM. *Appl Catal B: Environ* 2000; 25:181.

[24] Audisio G, Bertini F, Beltrame PL, Carniti P. *Makromol Chem Macromol Symp* 1992;57:191.

[25] Nanbu H, Sakuma Y, Ishihara Y, Takesue T, Ikemura T. *Polymer Degrad Stab* 1987;19:61.

[26] Corma A, Fornes V, Navarro MT, Perez-Pariente J. *J Catal* 1994;148:569.

[27] Ogawa T, Kuroki T, Ide S. *J Appl Polymer Sci* 1981; 27:857.

[28] Freeman ES, Carrol B. *J Physical Chemistry* 1958; 62:394.